



Research paper

Exploring structural properties of potent human carbonic anhydrase inhibitors bearing a 4-(cycloalkylamino-1-carbonyl) benzenesulfonamide moiety

Maria Rosa Buemi ^{a,1}, Anna Di Fiore ^{b,1}, Laura De Luca ^a, Andrea Angeli ^c,
 Francesca Mancuso ^a, Stefania Ferro ^a, Simona Maria Monti ^b, Martina Buonanno ^b,
 Emilio Russo ^d, Giovanbattista De Sarro ^d, Giuseppina De Simone ^b, Claudiu T. Supuran ^c,
 Rosaria Gitto ^{a,*}

^a Dipartimento di Scienze Chimiche, Biologiche, Farmaceutiche ed Ambientali (CHIBIOFARAM), Università degli Studi di Messina, Viale Palatucci, Polo didattico SS, Annunziata, 98168, Messina, Italy

^b Istituto di Biostrutture e Bioimmagini-CNR, Via Mezzocannone 16, 80134, Napoli, Italy

^c Dipartimento NEUROFARBA, Università di Firenze, Via Ugo Schiff 6, 50019, Sesto Fiorentino, Italy

^d Pharmacology Chair, Dept. of Science of Health School of Medicine, University of Catanzaro, Campus Universitario "Salvatore Venuta", Viale Europa - Loc. Germaneto, 88100, Catanzaro, Italy

ARTICLE INFO

Article history:

Received 7 September 2018

Received in revised form

13 November 2018

Accepted 29 November 2018

Available online 1 December 2018

Keywords:

Carbonic anhydrases

CA inhibitors

Benzenesulfonamides

X-ray crystallography

ABSTRACT

Guided by the crystal structure of 4-(3,4-dihydroquinolin-1(2H)-ylcarbonyl)benzenesulfonamide **3** in complex with hCA II (PDB code 4Z0Q), a novel series of cycloalkylamino-1-carbonylbenzenesulfonamides was designed and synthesized. Thus, we replaced the quinoline ring with an azepine/piperidine/piperazine nucleus and introduced further modifications on cycloalkylamine nucleus by means the installation of hydrophobic/hydrophilic functionalities able to establish additional contacts in the middle area of the enzyme cavity. Among the synthesized compounds, the derivatives **7a**, **7b**, **8b** exhibited a remarkable inhibition for hCA II and the brain-expressed hCA VII in subnanomolar range. The binding of these molecules to the target enzymes was characterized by means of a crystallographic analysis, providing a clear snapshot of the most important interactions established by this class of inhibitors into the hCA II and hCA VII catalytic site. Notably, our results showed that the benzylpiperazine tail of compound **8b** is oriented both in hCA II and in hCA VII toward a poorly explored region of the active site. These features should be further investigated for the design of new isoform selective CA inhibitors.

© 2018 Elsevier Masson SAS. All rights reserved.

1. Introduction

Human Carbonic Anhydrases (hCAs, EC 4.2.1.1) are zinc-containing enzymes, which catalyze a very simple reaction: the reversible hydration of carbon dioxide in bicarbonate and proton [1]. Twelve catalytically active isoforms have been so far identified that based on the different cellular distribution can be grouped in

four different classes: cytosolic (CA I, II, III, VII and XIII), mitochondrial (CA VA and VB), secretory (CA VI), and membrane associated (CA IV, IX, XII and XIV) CAs [2–5]. These isoforms differ also for catalytic efficiency and tissue distribution [6]. Several CA-isoforms play important roles in different pathological processes related to cancer, epilepsy, obesity, glaucoma, etc [7–14]. Therefore, these enzymes have become relevant targets for the design of inhibitors with biomedical applications. In details, hCA II and hCA VII are involved in GABA-mediated neuronal excitation [15], hCA IX and hCA XII have been characterized as tumor markers [8,10], whereas hCA XIV seems to play an important role in modulating excitatory synaptic transmission [16]. Four different classes of CA inhibitors (CAIs) [1] have been characterized so far: molecules that bind to the catalytic zinc ion, molecules anchoring to the zinc-coordinated water molecule/hydroxide ion, compounds occluding

Abbreviations: AAZ, acetazolamide; CA, carbonic anhydrase; CAI, carbonic anhydrase inhibitors; PTZ, pentylenetetrazole; TPM, topiramate.

* Corresponding author.

E-mail address: rgitto@unime.it (R. Gitto).

¹ These authors contributed equally to the work. The manuscript was written through contributions of all authors. All authors have given approval to the final version of the manuscript.

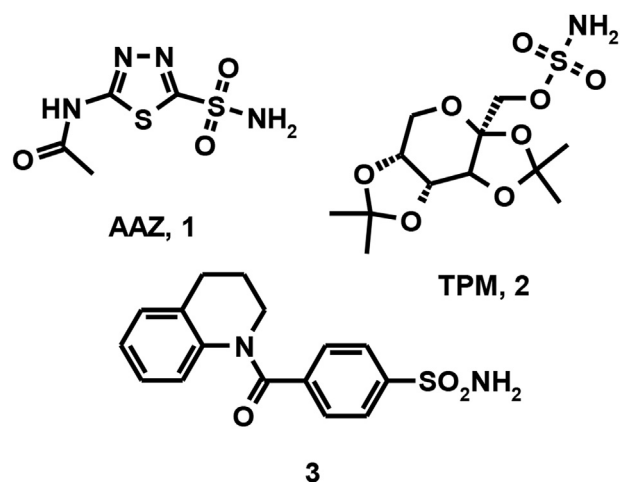


Chart 1. Chemical structures of well-known hCAs (1–2) and 4-(3,4-dihydroquinolin-1(2H)-ylcarbonyl)benzenesulfonamide (3).

the active site entrance, and compounds binding out of the active site. Among them, the most investigated CAIs are those possessing a sulfonamide/sulfamate zinc binder group (ZBG), of which acetazolamide (AAZ, **1**) and topiramate (TPM, **2**) (Chart 1) are two clinically used representatives.

It is well known that the presence of benzenesulfonamide as ZBG provides potent CAIs, whereas the affinity towards the different isoforms can be tuned by the nature of additional chemical fragment linked to benzenesulfonamide moiety [17]. In the course of our efforts to identify novel selective CAIs we have synthesized and tested a series of quinolone/isoquinoline-arylsulfonamides showing high affinity toward hCAs [11,18–26]. Among them, we have recently reported the discovery of a set of heterocyclic-*N*-carbonylbenzenesulfonamides as a class of potent inhibitors of druggable CA isoforms (hCA II, hCA VII, hCA IX and hCA XIV) as found for our prototype 4-(3,4-dihydroquinolin-1(2H)-ylcarbonyl)benzenesulfonamide **3** (Chart 1) [18,23,26,27]. To decipher the mode of action of these molecules we analyzed the crystal structures of several derivatives in complex with hCA II, thus identifying the network of interactions in the CA cavity [17]. Interestingly, the high resolution crystal structure of the hCA II/3 adduct (PDB code 4Z0Q) revealed that the benzenesulfonamide portion of the inhibitor is well anchored to the active site cavity establishing many stabilizing interactions with enzyme residues, whereas the heterocyclic fragment shows a high level of conformational flexibility. With the aim to improve our knowledge about the structure-affinity relationships (SARs) of CAIs bearing a benzenesulfonamide moiety, we designed a new class of compounds strictly related to the prototype **3**, containing azepine/piperidine/piperazine nucleus in place of the quinoline ring. Our design was based on the visual inspection of the binding pose in the hCA II active site for compound **3** for which the heterocyclic portion was positioned into the hydrophobic region formed by residues Phe131 and Pro202. Therefore, we have decorated the cycloalkylamine core with hydrophobic substituents able to establish additional contacts in the middle area of CA cavity thus controlling affinity and isoform selectivity toward several druggable CA isoforms, for which we addressed our biological screening by a stopped flow CO₂ hydration assay. Then, X-ray crystallography has been employed to get information on action mechanism of the newly designed molecules. Finally, we evaluated the ability of the most promising and selective hCA VII inhibitors to exert effects in pentylenetetrazole (PTZ) seizure tests as an *in vivo* model of epilepsy.

2. Results and discussion

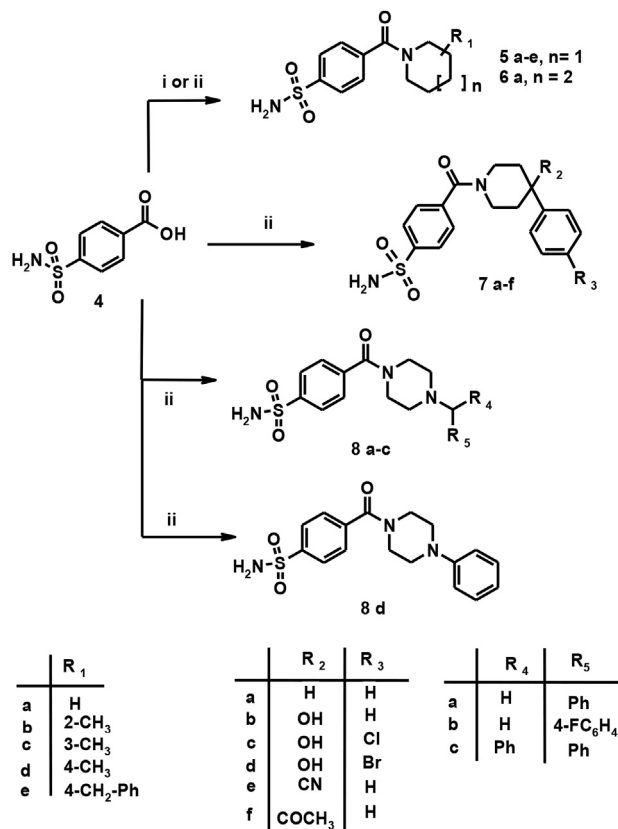
2.1. Chemistry

By coupling the commercially available 4-sulfamoylbenzoic acid (**4**) and suitable cycloalkylamines, the title 4-(piperidine-1-carbonyl)benzenesulfonamides (**5 a–e**), 4-(azepane-1-carbonyl)benzenesulfonamide (**6a**), 4-(4-phenylpiperidine-1-carbonyl)benzenesulfonamides (**7 a–f**), 4-(4-benzylpiperazine-1-carbonyl)benzenesulfonamides (**8 a–c**), and 4-(4-phenylpiperazine-1-carbonyl)benzenesulfonamide (**8 d**) have been readily obtained (Scheme 1).

This reaction was generally carried out at room temperature, in alkaline medium and in presence of *N,N,N,N*-tetramethyl-*O*-(1*H*-benzotriazol-1-yl)uronium hexafluorophosphate (HBTU) (pathway ii) except for compounds **5a** and **5d** for which carbonylimidazole (pathway i) was used to optimize the yield. The chemical characterization of arylsulfonamides **5 a–e**, **6a**, **7 a–f**, and **8 a–d** was supported by elemental analyses and spectroscopic measurements. ¹H NMR spectra data of representative compounds are shown in Supporting Material. In the ¹H NMR spectra of all studied compounds the aromatic and aliphatic protons were observed in the expected regions. A distinguished feature of these spectra was the presence of the typical broad single peaks which were observed for cycloalkylamine protons. NMR signals for four protons of benzenesulfonamide motif appeared as doublets at 7.5 and 7.8 ppm while the two protons of –SONH₂ group was observed as broad single peak at 7.4 ppm.

2.2. CA inhibition assay

The CA inhibitory effects of all synthesized compounds **5 a–e**, **6**



Scheme 1. Reagents and conditions: i) carbonylimidazole (DCI), THF, r.t., 3h, then RR'NH, DMF r.t., 2h; ii) RR'NH, HBTU, DMF, TEA, r.t., overnight.

Table 1
K_i values (nM) against hCA I, hCA II, hCA VII, hCA IX, hCA XII and hCA XIV isoforms showed by derivatives **3**, **5 a-e**, **6a**, **7a-f**, **8a-d**, AAZ **1** and TPM **2**.

	K _i (nM) ^a					
	hCA I	hCA II	hCA VII	hCA IX	hCA XII	hCA XIV
5a	9.2	5.7	8.3	3.1	7.9	23.8
5b	4.4	0.63	4.6	2.6	7.8	31.4
5c	187	6.1	16.5	2.4	4.5	41.7
5d	7.7	0.79	6.9	3.4	3.1	13.7
5e	75.5	1.5	0.63	7.0	9.4	53.7
6a	85.0	3.8	13.3	16.8	2.7	37.9
7a	1.7	0.5	0.45	3.3	6.6	46.9
7b	9.3	0.6	2.6	22.6	7.8	52.5
7c	6.6	0.6	1.0	24.9	8.5	7.8
7d	6.3	0.7	0.55	4.7	8.1	7.7
7e	6.5	0.6	0.68	18.4	6.4	11.0
7f	7.7	0.6	4.4	3.1	59.4	29.8
8a	6.8	3.0	10.4	33.1	3.8	34.6
8b	0.69	0.5	7.8	45.1	5.6	15.2
8c	50.1	5.7	7.8	28.2	8.5	42.8
8d	91.1	2.0	9.5	4.8	7.3	41.5
1	250	12.1	2.5	25.8	5.7	41.0
2	250	10	0.9	58	ND	1460
3	78.6	6.8	8.5	9.4	ND	39.0

^a Errors in the range of ±10% of the reported value, from 3 different assays. Recombinant full-length hCA I, hCA II and hCA VII and catalytic domains of hCA IX, hCA XII and hCA XIV were used.

a, **7 a-f**, and **8 a-d** were measured for human CA I, CA II, CA VII, CA IX, CA XII and CA XIV by a stopped flow CO₂ hydration assay. The obtained results are summarized in Table 1 and compared with K_i values of prototype **3** and two well-known inhibitors AAZ **1** and TPM **2** as reference compounds. As shown in Table 1, the four 4-(piperidine-1-carbonyl)benzenesulfonamides (**5a-e**) and the superior cyclohomologous 4-(azepane-1-carbonyl)benzenesulfonamide (**6a**) displayed significant inhibitory effects towards all studied CA isoforms when compared to well-known inhibitors **1** and **2**.

They generally demonstrated high inhibitory activity at low nanomolar concentration, except for outlier compounds **5c**, **5e** and **6a** against hCA I. Moreover, these compounds reported in Table 1 were poorer inhibitors of hCA XIV in respect to other studied isoforms. By deleting the benzene fused ring of prototype **3** we increased the affinity toward hCA II by an order of magnitude for 4-(2-methylpiperidine-1-carbonyl)benzenesulfonamide (**5b**) and 4-(4-methylpiperidine-1-carbonyl)benzenesulfonamide (**5d**), suggesting an optimized orientation within hCA II active site cavity. Notably, for the 4-(4-benzylpiperidine-1-carbonyl)benzenesulfonamide (**5e**) an improvement of affinity toward druggable isoform hCA VII has been found (K_i value of 0.63 nM), thus suggesting a crucial role of additional 4-benzylpiperidine group to benzenesulfonamide moiety to address hCA VII selectivity.

As shown in Table 1, by incorporating a phenyl moiety at C-4 position of piperidine nucleus, a further increased affinity against hCA II was observed for compound **7a** in comparison with analogous **5a** (K_i values of 0.5 vs 5.7 nM) and hCA VII (K_i values of 0.45 nM vs 8.3 nM). By introducing additional hydroxyl group, nitrile or acetyl functionalities at C-4 position, no significant improvement of hCA II inhibition was observed; as result the SAR analysis was very flat for compounds **7 a-f** as hCA II inhibitors. In contrast, the affinity against hCA VII was optimized for compounds **7d** (R₁ = OH and R₂ = 4-BrC₆H₄) and **7e** (R₁ = CN and R₂ = Ph) showing K_i values of 0.55 and 0.68 nM, respectively.

Notably, compounds **7a**, **7d** and **7e** demonstrated high inhibitory effects toward brain-distributed hCA VII with K_i values comparable to those of the anticonvulsant agent TPM **2**. For other studied isoforms, no clear correlation between K_i values and

structural modifications was observed for inhibitors **7 a-f**. The screening of piperazinyl derivatives **8 a-d** revealed that all compounds generally displayed inhibitory effects towards studied isoforms at nanomolar concentration. It appears that the installation of a 4-fluorobenzyl moiety optimizes the affinity toward hCA I and hCA II isoforms for compound **8b**.

2.3. In vivo testing

To evaluate the *in vivo* effects of the most efficacious inhibitors **7a**, **7d**, **8b**, and **8c** against the brain expressed hCA VII isoform, we carried out additional pharmacological studies. Specifically, we studied the ability of these compounds to prevent seizures in mice using pentylenetetrazole (PTZ) as chemical convulsant agent. The four selected compounds were tested at the doses of 20 and 30 mg/kg that were chosen according to the knowledge that the ED₅₀ of TPM (**2**) and AAZ (**1**) in this model are comprised between 22 and 27 mg/kg [28]. Unfortunately, none of the tested compounds was able to prevent the occurrence of clonus, whereas **2** protects against PTZ-induced shocks and convulsions [28]. At the dose of 20 mg/kg of tested compounds, some signs of sedation were observed, and this effect was confirmed at the higher dose of 30 mg/kg by which animals were clearly sedated. We thought that this event could be related to a toxic effect, therefore no higher doses were used. Considering latency to clonus (time to reach a stage 3 seizure after PTZ administration), all compounds were able to increase significantly (p < 0.05) this parameter, although no significant differences were observed at the doses and between the tested molecules. All tested compounds seem to have some effects on neuronal activity considering the signs of sedation and the increase in latency; however, the unexpected *in vivo* effects limit further detailed studies in this model. The lack of anticonvulsant effect suggests that the hCA VII inhibitory properties do not produce antiepileptic activity for this class of compounds at tested doses. However, we cannot exclude that a pharmacological effect could have onset at higher concentrations.

2.4. Structural analysis

To better characterize the inhibition mechanism of the newly designed and synthesized compounds, we solved the crystal structures of adducts that some representative molecules of the series, namely **7a**, **7b** and **8b**, form with isozymes hCA II and hCA VII. The data collection and refinement statistics for these six crystal structures are summarized in Table 2 and deposited in to PDB under codes 6H2Z, 6H33, 6H34, 6H36, 6H37 and 6H38.

Since compounds **7a-7f** displayed very high inhibitory activity against hCA II and hCA VII with respect to the prototype **3**, we initially solved the crystallographic structure of the lead compound **7a** in complex with both enzymes. Inspection of (Fo-Fc) and (2Fo-Fc) electron density maps at various stages of the crystallographic refinement showed features compatible with the presence of compound **7a** within the active site of both hCA II and hCA VII (Fig. 1A and B).

These maps were very well defined in both cases, thus indicating absence of inhibitor flexibility within enzyme active sites, differently from what observed for the prototype **3** within the hCA II active site [17]. As commonly observed for sulfonamide-based hCA inhibitors, in both adducts compound **7a** was anchored to the catalytic zinc ion via the primary sulfonamide group, displacing the zinc-bound solvent molecule and forming hydrogen bond interactions with Thr199 (Fig. 2A and B) [1]. The benzenesulfonamide core established strong hydrophobic interactions (distance < 4.0 Å) with residues His94, Leu198 and Val121 in the case of hCA II and with His94, Val121, Leu198 and Thr200 in the case of hCA VII (Fig. 2A and B).

Table 2
Data collection statistics and refinement statistics.

	hCA II in complex with			hCA VII in complex with		
	7a	7b	8b	7a	7b	8b
Cell parameters						
Space group	<i>P2₁</i>	<i>P2₁</i>	<i>P2₁</i>	<i>P2₁2₁2</i>	<i>P2₁2₁2</i>	<i>P2₁2₁2</i>
Cell dimensions (Å, °)	a = 42.4 b = 41.1 c = 71.7 β = 104.2	a = 42.3 b = 41.4 c = 72.0 β = 104.2	a = 42.3 b = 41.3 c = 72.1 β = 104.3	a = 66.0 b = 88.1 c = 44.0	a = 66.0 b = 88.6 c = 44.1	a = 66.1 b = 89.2 c = 44.2
Number of independent molecules	1	1	1	1	1	1
Data collection statistics						
Resolution limits (Å)	34.7–1.94	29.1–1.58	29.1–1.55	31.1–1.85	30.9–1.90	34.0–1.70
Total reflections	70015	136858	121412	91414	69324	138766
Unique reflections	17564	30160	33156	21202	19303	28527
Redundancy	4.0	4.5	3.7	4.3	3.6	4.9
Completeness (%)	98.6 (90.2)	90.7 (77.2)	93.8 (82.5)	94.1 (88.9)	92.1 (69.4)	96.6 (90.2)
R-merge*	0.114 (0.418)	0.045 (0.147)	0.055 (0.228)	0.067 (0.459)	0.046 (0.181)	0.046 (0.503)
Rmeas [§]	0.131 (0.521)	0.050 (0.173)	0.062 (0.280)	0.074 (0.573)	0.052 (0.213)	0.051 (0.590)
Rpim [¶]	0.063 (0.306)	0.021 (0.089)	0.028 (0.161)	0.032 (0.338)	0.024 (0.108)	0.021 (0.301)
<I>/<σ(I)>	11.5 (2.3)	29.9 (9.0)	21.8 (4.4)	18.0 (2.2)	22.3 (7.4)	27.3 (2.6)
Refinement statistics						
Resolution limits (Å)	34.7–1.94	29.1–1.58	29.1–1.55	31.1–1.85	30.9–1.90	34.0–1.70
R-work** (%)	17.9	16.6	17.1	19.5	19.4	19.3
R-free** (%)	21.4	19.4	20.6	23.3	23.6	24.5
r.m.s.d. from ideal geometry:						
Bond lengths (Å)	0.006	0.008	0.009	0.008	0.007	0.006
Bond angles (°)	1.4	1.5	1.6	1.5	1.5	1.5
Number of protein atoms	2039	2093	2063	2066	2057	2055
Number of inhibitor atoms	24	25	26	24	25	26
Number of water molecules	158	225	229	116	115	144
Average B factor (Å ²)						
All atoms	16.04	12.51	11.88	22.91	19.45	21.27
Protein atoms	15.42	11.52	10.78	22.61	19.22	20.75
Inhibitor atoms	16.97	15.50	20.29	21.45	19.60	19.92
Waters	23.30	21.33	20.57	28.68	23.68	28.32
PDB accession code	6H2Z	6H33	6H34	6H36	6H37	6H38

*R-merge = $\sum_{hkl} \sum_i |I_i(hkl) - \langle I(hkl) \rangle| / \sum_{hkl} \sum_i I_i(hkl)$, where $I_i(hkl)$ is the intensity of an observation and $\langle I(hkl) \rangle$ is the mean value for its unique reflection; summations are over all reflections; $§Rmeas = \sum_{hkl} \{N(hkl) / [N(hkl) - 1]\}^{1/2} \times \sum_i |I_i(hkl) - \langle I(hkl) \rangle| / \sum_{hkl} \sum_i I_i(hkl)$; $¶Rpim = \sum_{hkl} \{1 / [N(hkl) - 1]\}^{1/2} \times \sum_i |I_i(hkl) - \langle I(hkl) \rangle| / \sum_{hkl} \sum_i I_i(hkl)$; ****R-work = $\sum_{hkl} ||F_o(hkl)| - |F_c(hkl)|| / \sum_{hkl} |F_o(hkl)|$** calculated for the working set of reflections. R-free is calculated as for R-work, but from data of the test set that was not used for refinement (Test Set Size (%) = 5.7% for hCA II/**7a**, 3.5% for hCA II/**7b**, 3.0% for hCA II/**8b**, 5.0% for hCA VII/**7a** and hCA VII/**7b**, 4.0% for hCA VII/**8b**). Values in parentheses are referred to the highest resolution shell (2.01–1.94 Å for hCA II/**7a**, 1.64–1.58 Å for hCA II/**7b** and 1.61–1.55 Å for hCA II/**8b**, 1.92–1.85 Å for hCA VII/**7a**, 1.97–1.90 Å for hCA VII/**7b**, 1.76–1.70 Å for hCA VII/**8a**).

Moreover, the carbonyl group was hydrogen bonded to Gln92 in the hCA VII active site, but not in the case of hCA II. Finally, 4-phenylpiperidine substituent was oriented both in hCA II and in hCA VII toward the hydrophobic region of the active site establishing many hydrophobic interactions with enzyme residues. Overall, the interactions established by **7a** with the two isoforms were very similar, with the exception of the hydrogen bond, which the inhibitor formed with Gln92 in hCA VII. However, it appears that this hydrogen bond does not contribute significantly to the binding affinity since the K_i values of the inhibitor against the two enzymes are comparable. We also studied compound **7b** bearing an additional hydroxyl group at C-4 position to respect parent compound **7a**; it has been found that the installation of a polar moiety did not cause significant changes in the interaction mode of the inhibitor with hCA II and hCA VII active sites (Fig. 1C, D, 2C and 2D) when compared with compound **7a**. This evidence results in good agreement with the very similar K_i values against hCA II (0.5 nM and 0.6 nM for **7a** and **7b**, respectively); whereas the slight divergence found for K_i values against hCA VII (0.45 nM and 2.6 nM for **7a** and **7b**, respectively) are not consistent with their very similar binding pose within the hCA II and hCA VII active sites. Thus, we can speculate that the higher affinity of **7a** with respect to **7b** for the brain enzyme has to probably be ascribed to other molecular factors that cannot be detected by crystallographic studies.

Finally, to investigate on the binding mode of the piperazine derivatives we solved the structure of one of the most active

molecules of the series, namely compound **8b**, in complex with hCA II and hCA VII. Surprisingly, despite kinetic experiments indicated for this molecule a higher binding affinity for hCA II with respect to hCA VII, the electron density maps of the inhibitor were better defined in the case of the adduct with the brain enzyme with respect to the adduct with the ubiquitous hCA II (Fig. 1E and F). The analysis of the structures of the two adducts provided an explanation to this apparent inconsistency. Indeed, in both cases the inhibitor is bound to the enzyme active site establishing the canonical interactions of the benzenesulfonamide moiety with CA active site. Moreover, polar and hydrophobic interactions between the phenyl-carbonyl-piperazine moieties and residues which delimit the cavity (see Fig. 3A and B) are detectable. However, in the case of hCA VII/**8b** adduct, additional interactions are established between the inhibitor and residue R159 of a symmetry-related molecule. Thus, it is evident that the lower conformational flexibility of **8b** in hCA VII active site is related to the crystal packing and thus it is not present in solution.

Finally, it is worth noting that both in hCA II/**8b** and in hCA VII/**8b** the benzylpiperazine tail is oriented toward a rather unexplored region of the active site located at the border of its hydrophobic portion (Fig. 4) [29]. Indeed, it has been reported that the majority of hCAs orient their tail toward either the hydrophobic or the hydrophilic region of the catalytic cavity [1,33]. Due to this unusual feature, these piperazine-derivatives should be further investigated to address selectivity issues.

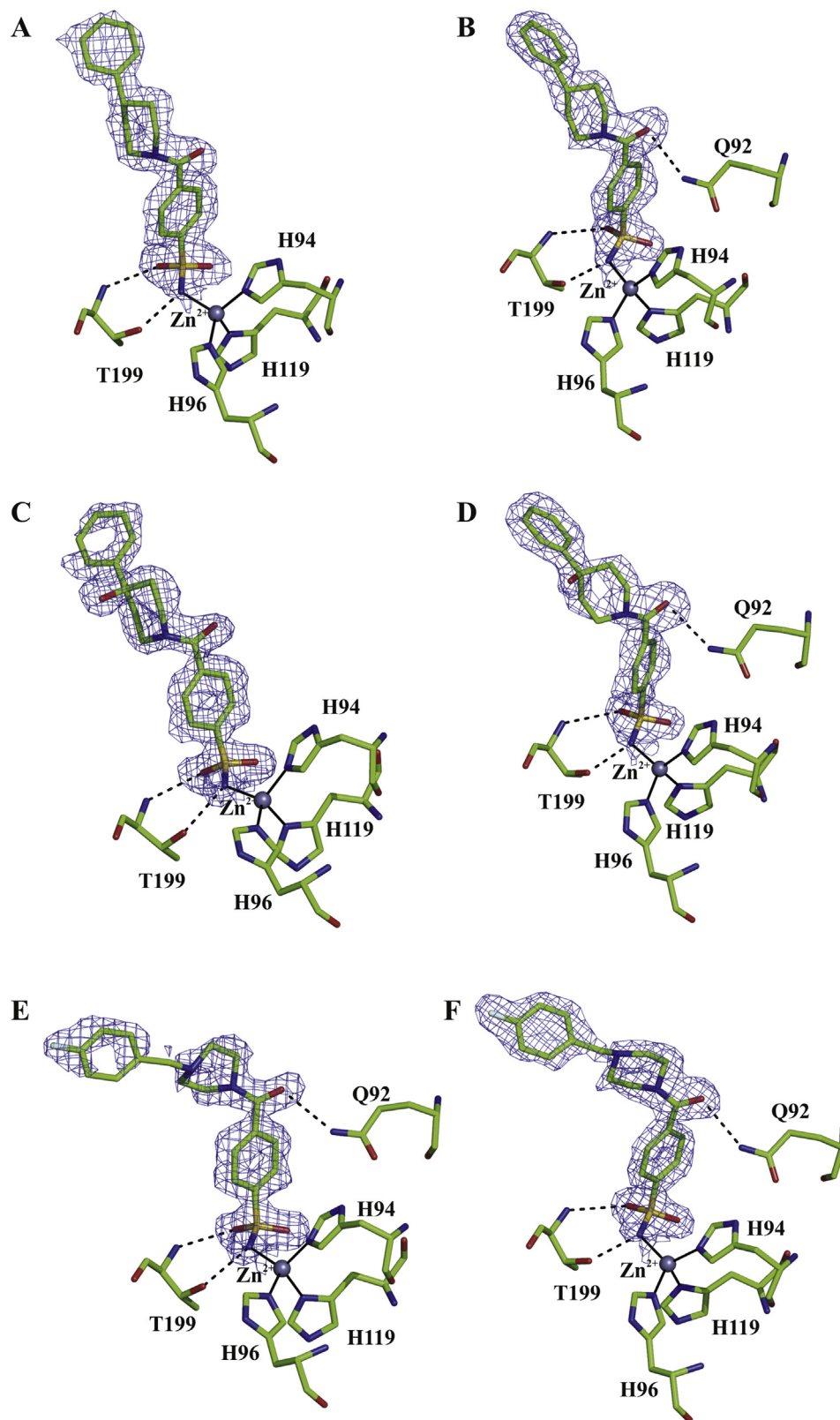


Fig. 1. Electron density of inhibitors. Sigma-A weighted $|2F_o - F_c|$ simulated annealing omit map of inhibitors bound in hCA II and hCA VII active sites. A) hCA II/7a, B) hCA VII/7a, C) hCA II/7b, D) hCA VII/7b, E) hCA II/8b and F) hCA VII/8b. Zinc ion is represented as a gray sphere. The figure is contoured to the 1.0 σ level and was generated by using PyMOL (<https://pymol.org>).

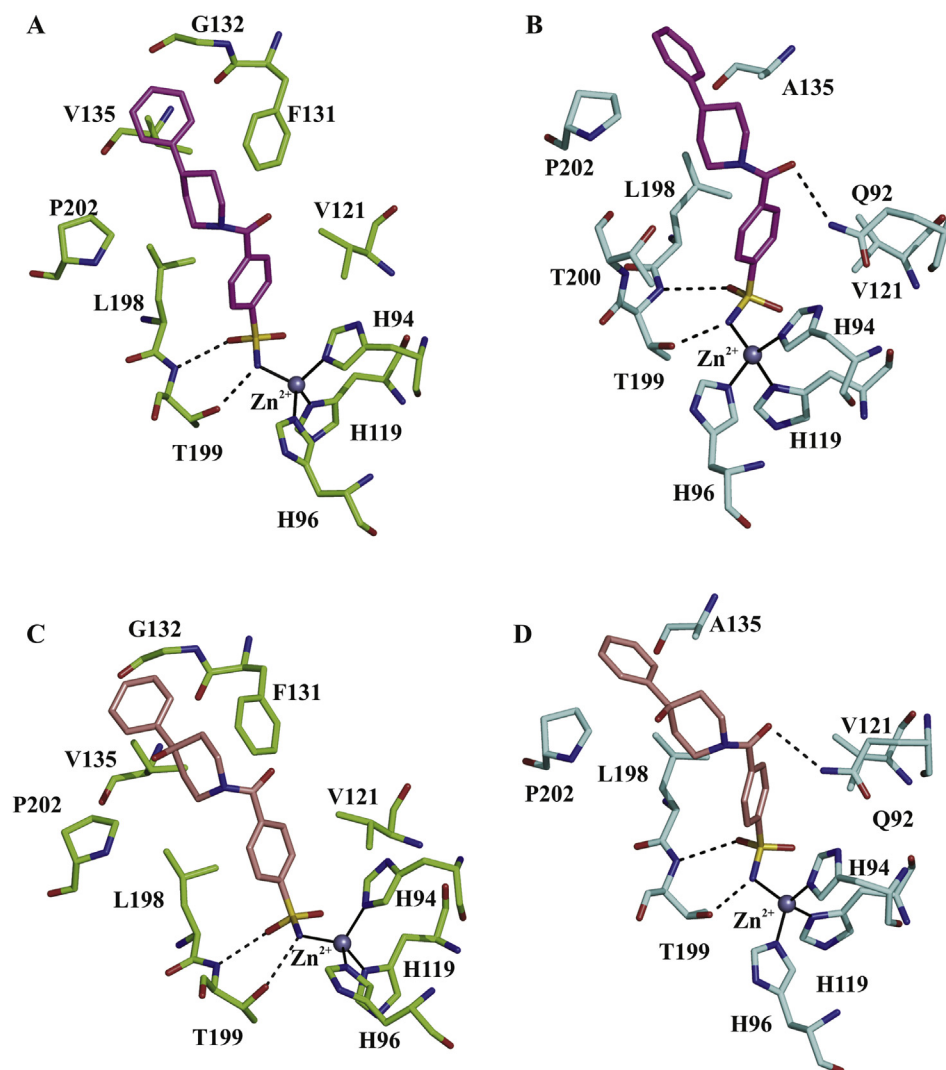


Fig. 2. Piperidine-1-carbonyl-benzenesulfonamides bound to the active site of hCA II (green) and hCA VII (cyan). A and B: compound **7a** (magenta). C and D: compound **7b** (salmon). Residues involved in hydrophobic interactions and hydrogen bonds (black dashed lines) are shown. The figure was made using PyMol. (For interpretation of the references to color in this figure legend, the reader is referred to the Web version of this article.)

3. Conclusions

In conclusion, a series of new 4-(cycloalkylamino-1-carbonyl) benzenesulfonamide derivatives was synthesized and tested by a stopped flow CO₂ hydration assay. The most potent compounds demonstrated excellent inhibitory effects against several CA isozymes at subnanomolar concentration. The findings were corroborated by crystallographic structures of the hit compounds in complex with hCAII and hCA VII isoforms. Our structural investigation confirmed that the combination of the crucial benzenesulfonamide moiety with a suitable aromatic tail can offer the optimization of affinity toward both isoforms. Notably, we found that the rim of catalytic cavity of these isoforms might be exploited to reinforce the network of interactions. Overall, we envision that these structural information for hCA VII adducts will furnish suggestions for design new potent and selective inhibitors against this brain-expressed CA isoform.

4. Experimental section

4.1. Chemistry

All reagents were used without further purification and bought

from common commercial suppliers. Microwave-assisted reactions were carried out in a Focused Microwave TM Synthesis System, Model Discover (CEM Technology Ltd Buckingham, UK). Melting points were determined on a Buchi B-545 apparatus (BUCHI Labortechnik AG Flawil, Switzerland) and are uncorrected. By combustion analysis (C, H, N) carried out on a Carlo Erba Model 1106-Elemental Analyzer we determined the purity of synthesized compounds; the results confirmed a $\geq 95\%$ purity. Merck Silica Gel 60 F254 plates were used for analytical TLC (Merck KGaA, Darmstadt, Germany). For detection, iodine vapor and UV light (254 nm) were used. Flash Chromatography (FC) was carried out on a Biotage SP1 EXP (Biotage AB Uppsala, Sweden). ¹H NMR and ¹³C NMR spectra were measured in dimethylsulfoxide-d₆ (DMSO-d₆) and CDCl₃ with a Varian Gemini 300 spectrometer (Varian Inc. Palo Alto, California USA); chemical shifts are expressed in δ (ppm) and coupling constants (*J*) in hertz. All exchangeable protons were confirmed by addition of D₂O. R_f values were determined on TLC plates using a mixture of DCM/MeOH (96/4) as eluent.

4.1.1. Synthetic procedures for compounds **5 a-e**, **6a**, **7 a-f**, **8 a-d**

Pathway i: To a solution of 4-(aminosulfonyl)benzoic acid (**4**) (6 mmol) in THF (15 mL) the carbonylimidazole (6 mmol) (CDI) at

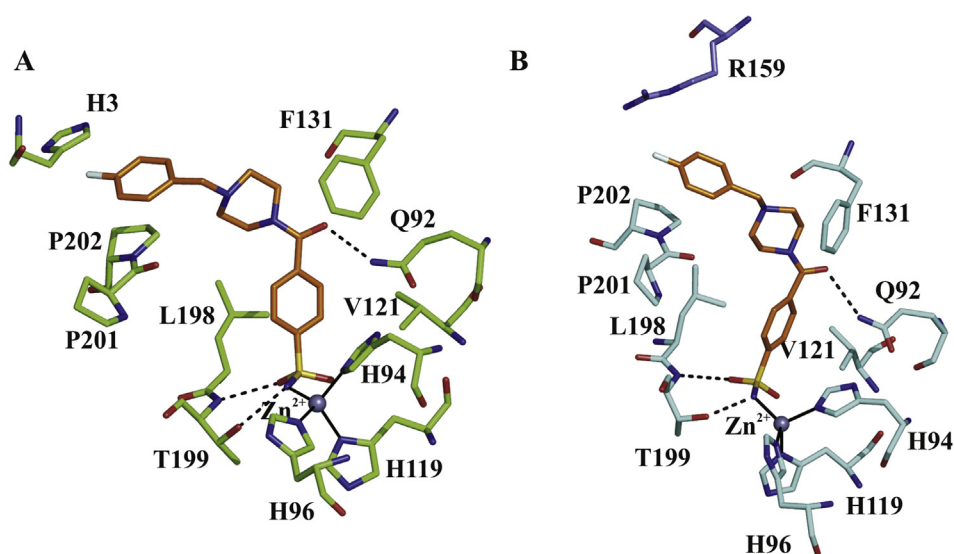


Fig. 3. (4-Fluorophenyl-piperazine-1-carbonyl)benzenesulfonamide **8b** (orange) bound to the active site of hCA II (green) (A) and hCA VII (cyan) (B). Residues involved in hydrophobic interactions and hydrogen bonds (black dashed lines) are shown. In (B) residue R159 belonging to a symmetry-related molecule is colored in violet. The figure was made by using PyMol. (For interpretation of the references to color in this figure legend, the reader is referred to the Web version of this article.)

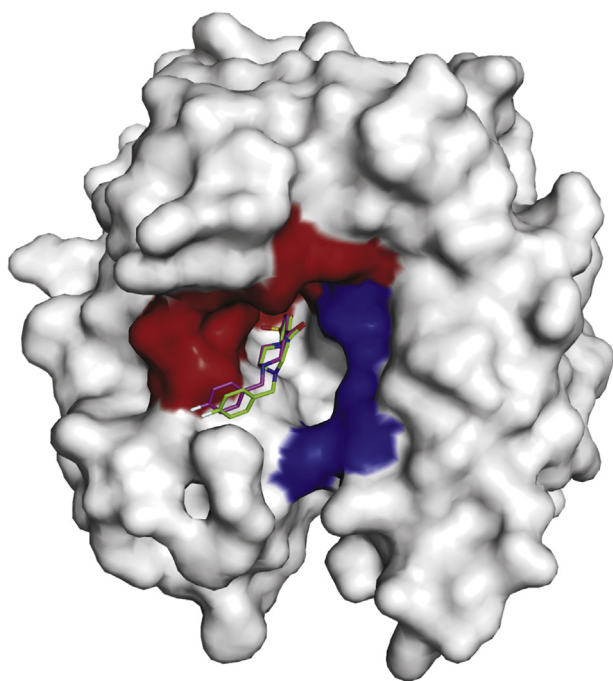


Fig. 4. Structural superposition of compound **8b** when bound to hCA II (green) with the same compound when bound to hCA VII (magenta). The surface representation of hCA II is also shown with hydrophobic region of the active site in red and the hydrophilic one in blue. The figure was made using PyMol. (For interpretation of the references to color in this figure legend, the reader is referred to the Web version of this article.)

0 °C was added. The obtained mixture was stirred at room temperature for 3h and then the appropriate amine derivative (15 mmol) in DMF (5 mL) was added dropwise. The reaction mixture was stirred at room temperature for 2h. The solvent was removed in vacuo; by adding of aqueous solution of NaHCO₃ (5 mL) we obtained compounds **5a** and **5d** as crude products, which were purified through crystallization by a mixture of Et₂O and EtOH (1:1).

Pathway ii: A mixture of 4-(aminosulfonyl)benzoic acid (**4**) (2 mmol) and N,N,N,N-tetramethyl-O-(1H-benzotriazol-1-yl)uranyl hexafluorophosphate (HBTU) (2 mmol) in DMF (2 mL) was stirred at room temperature for 1 h. Then, a solution of the appropriate amine derivative (2 mmol) in TEA (2 mmol) was added dropwise. The reaction mixture was left overnight and then quenched with water (10 mL) and extracted with EtOAc (3 × 5 mL). The organic phase was dried with Na₂SO₄ and the solvent was removed in vacuo. The residue was purified by flash chromatography (DCM/MeOH 96:4), crystallized by treatment with a mixture of Et₂O and EtOH (1:1) to give the desired final compounds **5b**, **5c**, **6a**, **7a-f** and **8a-d** as white crystals. For compounds **5a-d**, **6a**, **8a** and **8d** registered CAS numbers have been already assigned. However, their synthetic procedures, chemical properties and structural characterization are not available in literature.

4.1.1.1. 4-(Piperidine-1-carbonyl)benzenesulfonamide (5a); CAS:4302-78-7. Yield: 40%; M.p.: 206–207 °C; R_f = 0.45. ¹H NMR (DMSO-*d*₆): (δ) 1.43–3.57 (m, 10H), 7.45 (bs, 2H, NH₂), 7.53 (d, *J* = 8.2, 2H, ArH), 7.83 (d, *J* = 8.2, 2H, ArH). Anal. Calcd for C₁₂H₁₆N₂O₃S: C: 53.71; H: 6.01; N: 10.44. Found: C: 53.81; H: 6.11; N 10.54.

4.1.1.2. 4-(2-Methylpiperidine-1-carbonyl)benzenesulfonamide (5b); CAS 1097096-08-6. Yield: 60%; M.p.: 186–187 °C; R_f = 0.47. ¹H NMR (DMSO-*d*₆): (δ) 1.15 (d, *J* = 7.1, 3H, CH₃), 1.43–3.40 (m, 9H), 7.42 (bs, 2H, NH₂), 7.50 (d, *J* = 8.2, 2H, ArH), 7.83 (d, *J* = 8.2, 2H, ArH). Anal. Calc for C₁₃H₁₈N₂O₃S: C: 55.30; H: 6.43; N: 9.92. Found: C: 55.35; H: 6.40; N: 9.97.

4.1.1.3. 4-(3-Methylpiperidine-1-carbonyl)benzenesulfonamide (5c); CAS 4367-75-3. Yield: 35%; M.p.: 190–191 °C; R_f = 0.49. ¹H NMR (DMSO-*d*₆): (δ) 1.06 (d, *J* = 7.1, 3H, CH₃), 1.10–2.94 (m, 9H), 7.43 (bs, 2H, NH₂), 7.52 (d, *J* = 8.2, 2H, ArH), 7.84 (d, *J* = 8.2, 2H, ArH). Anal. Calcd for C₁₃H₁₈N₂O₃S: C: 55.30; H: 6.43; N: 9.92. Found: C: 55.40; H: 6.53; N: 10.02.

4.1.1.4. 4-(4-Methylpiperidine-1-carbonyl)benzenesulfonamide (5d); CAS 1096951-92-6. Yield: 40%; M.p.: 212–213 °C; R_f = 0.51. ¹H NMR (DMSO-*d*₆): (δ) 0.90 (d, *J* = 7.0, 3H, CH₃), 1.06–4.44 (m, 9H), 7.44 (bs, 2H, NH₂), 7.53 (d, *J* = 8.2, 2H, ArH), 7.84 (d, *J* = 8.2,

2H, ArH). Anal. Calcd for $C_{13}H_{18}N_2O_3S$: C:55.30; H:6.43; N:9.92. Found: C:55.40; H:6.40; N:9.80.

4.1.1.5. 4-(4-Benzylpiperidine-1-carbonyl)benzenesulfonamide (**5e**). Yield 44%; M.p.: 156–157 °C; $R_f = 0.59$. 1H NMR (DMSO- d_6): (δ) 1.12–1.66 (m, 4H), 2.52 (m, 2H, CH_2Ph), 2.62–2.44 (m, 5H), 7.15–7.16 (m, 3H, ArH), 7.24–7.27 (m, 2H, ArH), 7.42 (bs, 2H, NH_2), 7.52 (d, $J = 8.2$, 2H, ArH), 7.84 (d, $J = 8.2$, 2H, ArH). Anal. Calcd for $C_{19}H_{22}N_2O_3S$: C:63.66; H:6.19; N:7.81. Found: C:63.56; H:6.09; N:7.71.

4.1.1.6. 4-(Azepane-1-carbonyl)benzenesulfonamide (**6a**) CAS **1015627–49–2**. Yield: 30%; M.p.: 200–201 °C; $R_f = 0.53$. 1H NMR (DMSO- d_6): (δ) 1.50–3.53 (m, 12H), 7.43 (bs, 2H, NH_2), 7.51 (d, $J = 7.6$, 2H, ArH), 7.83 (d, $J = 7.6$, 2H, ArH). Anal. Calcd for $C_{13}H_{18}N_2O_3S$: C:55.30; H:6.43; N:9.92. Found: C:55.40; H: 6.53, N:9.82.

4.1.1.7. 4-(4-Phenylpiperidine-1-carbonyl)benzenesulfonamide (**7a**). Yield: 73%; M.p.: 222–223 °C; $R_f = 0.55$. 1H NMR (DMSO- d_6): (δ) 1.86–4.60 (m, 9H), 7.18–7.28 (m, 5H, ArH), 7.45 (s, 2H, NH_2), 7.61 (d, $J = 8.00$, 2H, ArH), 7.86 (d, $J = 8.00$, 2H, ArH). Anal. Calcd for $C_{18}H_{20}N_2O_3S$: C:62.77; H:5.85; N:8.13. Found: C:63.10; H:5.65; N:8.47.

4.1.1.8. 4-(4-Hydroxy-4-phenylpiperidine-1-carbonyl)benzenesulfonamide (**7b**). Yield: 34%; M.p.: 135–137 °C; $R_f = 0.37$. 1H NMR (DMSO- d_6): (δ) 1.51–4.45 (m, 8H), 5.20 (bs, 1H, OH), 7.18–7.32 (m, 3H, ArH), 7.45 (bs, 2H, NH_2), 7.51 (m, 2H, ArH), 7.63 (d, $J = 8.2$, 2H, ArH), 7.86 (d, $J = 8.2$, 2H, ArH). Anal. Calcd for $C_{18}H_{20}N_2O_4S$: C:59.98; H:5.59; N:7.77. Found: C:60.18; H:5.79; N:7.87.

4.1.1.9. 4-[4-(4-Chlorophenyl)-4-hydroxypiperidine-1-carbonyl]benzenesulfonamide (**7c**). Yield: 31%; M.p.: 215–217 °C; $R_f = 0.38$. 1H NMR (DMSO- d_6): (δ) 1.52–4.44 (m, 8H), 5.31 (bs, 1H, OH), 7.36 (d, $J = 8.5$, 2H, ArH), 7.44 (bs, 2H, NH_2), 7.54 (d, $J = 8.5$, 2H, ArH), 7.63 (d, $J = 7.6$, 2H, ArH), 7.86 (d, $J = 7.6$, 2H, ArH). Anal. Calcd For $C_{18}H_{19}ClN_2O_4S$: C:54.75; H:4.85; N:7.09. Found: C:54.93; H:5.13; N:7.37.

4.1.1.10. 4-[4-(4-Bromophenyl)-4-hydroxy-piperidine-1-carbonyl]benzenesulfonamide (**7d**). Yield: 35%; M.p.: 219–220 °C; $R_f = 0.40$. 1H NMR (DMSO- d_6): (δ) 1.48–4.45 (m, 8H), 5.31 (s, 1H, OH), 7.44 (bs, 2H, NH_2), 7.49–7.52 (m, 4H, ArH), 7.65 (d, $J = 8.8$, 2H, ArH), 7.87 (d, $J = 8.8$, 2H, ArH). Anal. Calcd for $C_{18}H_{19}BrN_2O_4S$: C:49.21; H:4.36; N:6.38. Found: C:49.58; H:4.67; N:6.44.

4.1.1.11. 4-(4-Cyano-4-phenylpiperidine-1-carbonyl)benzenesulfonamide (**7e**). Yield: 22%; M.p.: 285–286 °C; $R_f = 0.59$. 1H NMR (DMSO- d_6): (δ) 2.07–4.67 (m, 8H), 7.35–7.42 (m, 3H, ArH), 7.42 (bs, 2H, NH_2), 7.45–7.47 (m, 4H, ArH), 7.66 (d, $J = 8.2$, 2H, ArH), 7.87 (d, $J = 8.2$, 2H, ArH). Anal. Calcd for $C_{19}H_{19}N_3O_3S$: C: 61.77; H:5.18; N:11.37. Found: C:6.83; H:5.47; N:11.62.

4.1.1.12. 4-(4-Acetyl-4-phenyl-piperidine-1-carbonyl)benzenesulfonamide (**7f**). Yield: 20%; M.p.: 233–234 °C; $R_f = 0.52$. 1H NMR (DMSO- d_6): (δ) 1.89 (s, 3H, CH_3), 1.96–3.92 (m, 8H), 7.28–7.38 (m, 5H, ArH), 7.44 (bs, 2H, NH_2), 7.55 (d, $J = 8.2$, 2H, ArH), 7.83 (d, $J = 8.2$, 2H, ArH). Anal. Calcd for $C_{20}H_{22}N_2O_4S$: C:62.16; H:5.74; N:7.25. Found: C:62.10; H:5.84; N:7.15.

4.1.1.13. 4-(4-Benzylpiperazine-1-carbonyl)benzenesulfonamide (**8a**); CAS **1032228–25–3**. Yield 40%; M.p.: 204–205 °C; $R_f = 0.43$. 1H NMR (DMSO- d_6): (δ) 2.32–3.60 (m, 8H), 3.47 (s, 2H, CH_2Ph), 7.22–7.26 (m, 5H, ArH), 7.44 (bs, 2H, NH_2), 7.56 (d, $J = 8.2$, 2H, ArH), 7.83 (d, $J = 8.2$, 2H, ArH). Anal. Calcd for $C_{18}H_{21}N_3O_3S$:

C:60.15; H:5.89; N:11.69. Found: C:60.25; H:5.99; N:11.99.

4.1.1.14. 4-[4-[(4-Fluorophenyl)methyl]piperazine-1-carbonyl]benzenesulfonamide (**8b**). Yield 30%; M.p. 206–207 °C; $R_f = 0.45$. 1H NMR (CDCl $_3$): (δ) 2.35–3.62 (m, 8H), 2.49 (s, 2H, CH_2Ph), 7.11–7.36 (m, 4H, ArH), 7.46 (bs, 2H, NH_2), 7.57 (d, $J = 8.2$, 2H, ArH), 7.85 (d, $J = 8.2$, 2H, ArH). Anal. Calcd for $C_{18}H_{20}FN_3O_3S$: C:57.28; H:5.34; N:11.13. Found: C:57.55; H:5.43; N:11.34.

4.1.1.15. 4-(4-Benzhydrylpiperazine-1-carbonyl)benzenesulfonamide (**8c**). Yield 60%; M.p.: 228–230 °C; $R_f = 0.58$. 1H NMR (DMSO- d_6): (δ) 2.26–4.32 (m, 9H), 7.16–7.39 (m, 10H, ArH), 7.41 (bs, 2H, NH_2), 7.52 (d, $J = 8.2$, 2H, ArH), 7.81 (d, $J = 8.2$, 2H, ArH). ^{13}C NMR (DMSO- d_6): (δ) 172.8, 149.9, 147.6, 144.14, 133.8, 132.8, 132.19, 131.08, 130.8, 79.9, 79.8. Anal. Calcd for $C_{24}H_{25}N_3O_3S$: C:66.18; H:5.79; N:9.65. Found: C:66.28; H:5.69; N:9.55.

4.1.1.16. 4-(4-Phenylpiperazine-1-carbonyl)benzenesulfonamide (**8d**); CAS **1015405–80–7**. Yield 84%; M.p.: 231–232 °C; $R_f = 0.59$. 1H NMR (DMSO- d_6): (δ) 3.10–3.89 (m, 8H), 6.80–7.24 (m, 5H, ArH), 7.42 (bs, 2H, NH_2), 7.58 (d, $J = 8.2$, 2H, ArH), 7.84 (d, $J = 8.2$, 2H, ArH). Anal. Calcd for $C_{17}H_{19}N_3O_3S$: C:59.11; H:5.54; N:12.16. Found: C:58.81; H:5.24; N:12.06.

4.2. CA inhibition assay

An Applied Photophysics stopped-flow instrument has been used for assaying the CA catalysed CO_2 hydration activity. Phenol red (at a concentration of 0.2 mM) has been used as indicator, working at the absorbance maximum of 557 nm, with 10–20 mM Hepes (pH 7.5) or Tris (pH 8.3) as buffers, and 20 mM Na_2SO_4 or 20 mM $NaClO_4$ (for maintaining constant the ionic strength), following the initial rates of the CA-catalysed CO_2 hydration reaction for a period of 10–100 s. The CO_2 concentrations ranged from 1.7 to 17 mM for the determination of the kinetic parameters and inhibition constants. For each inhibitor at least six traces of the initial 5–10% of the reaction have been used for determining the initial velocity. The uncatalyzed rates were determined in the same manner and subtracted from the total observed rates. Stock solutions of inhibitor (10 mM) were prepared in distilled-deionized water and dilutions up to 0.01 nM were done thereafter with distilled-deionized water. Inhibitor and enzyme solutions were preincubated together for 15 min at room temperature prior to assay, in order to allow for the formation of the E-I complex. The inhibition constants were obtained by non-linear least-squares methods using PRISM 3, as reported earlier, and represent the mean from at least three different determinations. CA isoforms were recombinant ones obtained as reported earlier by this group [30–32].

4.3. Anticonvulsant test

Male ICR CD-1 mice ($n = 80$) were purchased from Charles River Laboratories s.r.l. (Calco, Lecco, Italy). Animals were housed four/five per cage and kept under controlled environmental conditions ($60 \pm 5\%$ humidity; 22 ± 2 °C; 12/12 h reversed light/dark cycle; lights on at 20.00). Animals were allowed free access to standard laboratory chow and tap water. The study was approved by the local ethics committee and all procedures involving animals and their care were in compliance with international and national regulations (EU Directive 2010/63/EU for animal experiments, ARRIVE guidelines and the Basel declaration including the 3R concept). Male ICR CD-1 mice (30–35 g, 35–40 days old) were pretreated with vehicle or drugs (groups of 10 mice per dose) 30 min before the i.p. administration of pentylenetetrazole (PTZ) 60 mg/kg (inducing clonus in 80% of mice) in order to test the efficacy against

clonus, as previously described [28].

4.4. X-ray crystallography

Crystals of the hCA II-**7b** and hCA II-**8b** adducts were obtained by co-crystallization. In particular, complexes were prepared by adding a 5 M excess of the inhibitor to a 10 mg/mL protein solution. This mixture, equilibrated for 1 h at room temperature, was used for the crystallization experiments. Drops were prepared by mixing 1 μ l of enzyme/inhibitor solution with 1 μ l of precipitant solution containing 1.3 M sodium citrate, 0.1 M Tris–HCl, pH 8.5 and further equilibrated over a well containing 1 mL of precipitant buffer. Crystals appeared in the drops within 2–3 days and grew to a maximum dimension of $0.2 \times 0.3 \times 0.2$ mm³ in about one week. Crystals of the hCA II-**7a** adduct were instead obtained by using the soaking technique. In particular, native hCA II crystals were grown at room temperature by the hanging drop vapor diffusion technique using a protein concentration of 10 mg/mL and 1.3 M sodium citrate, 0.1 M Tris–HCl, pH 8.5 as precipitant solution. A few hCA II crystals were then transferred in a 2 μ l drop of freshly prepared precipitant solution containing also the inhibitor at the concentration of 2.5 mM and glycerol (15% v/v) as cryoprotectant. These crystals were kept in the soaking solution for one night and finally flash-frozen in liquid nitrogen. A very similar experimental strategy was used to obtain crystals of the hCA VII–inhibitor complexes. For crystallographic studies a mutated form of hCA VII, where the cysteine residues in position 183 and 217 were mutated to serines, was used, since we previously reported that this mutant was more suitable for crystallization experiments [33,34] hCA VII crystals were grown at room temperature by the vapor diffusion hanging drop method. Equal volumes of protein (5 mg/mL in 0.02 M Tris–HCl pH 8.0 and 0.1 M NaCl) and precipitant solutions (25% v/v Peg3350, 0.2 M Ammonium acetate and 0.1 M Tris pH 8.5) were mixed and equilibrated against 1 mL reservoir containing the same precipitant solution. A few crystals of hCA VII were then transferred into a 2 μ l drop of the freshly prepared precipitant solution containing the inhibitor at a concentration of 40 mM for inhibitors **7a** and **7b** and 10 mM for **8b**. Moreover, 25% (v/v) glycerol was used as cryoprotectant agent. These crystals were kept in the soaking solution overnight and then flash-frozen in a gaseous nitrogen stream prior to the diffraction experiment. All X-ray data sets were collected at 100 K by a copper rotating anode generator developed by Rigaku and equipped with a Rigaku Saturn CCD detector. Diffraction data were indexed, integrated and scaled using the HKL2000 software package [35]. Data collection statistics are reported in Table 2. The initial phases of all structures were calculated using the atomic coordinates of hCA VII and hCA II (PDB accession code 6G4T and 1CA2 for hCA VII and II, respectively) with waters removed [34–36]. The structures were refined using the CNS program [37,38] as previously described [39–41], whereas model building and map inspections were performed using the program O [42]. Topology files for inhibitors **7a**, **7b** e **8b** generated using the PRODRG server [43].

Notes

The authors declare no competing financial interest.

Acknowledgments

Financial support for this research by by Fondo di Ateneo per la Ricerca (PRA grant number ORME09SPNC - Università degli Studi di Messina. We thank Mr. Maurizio Amendola and Mr. Giosuè Sorrentino for their skillful technical assistance with X-ray measurements.

Appendix A. Supplementary data

Supplementary data to this article can be found online at <https://doi.org/10.1016/j.ejmech.2018.11.073>.

References

- [1] V. Alterio, A. Di Fiore, K. D'Ambrosio, C.T. Supuran, G. De Simone, Multiple binding modes of inhibitors to carbonic anhydrases: how to design specific drugs targeting 15 different isoforms? *Chem. Rev.* 112 (2012) 4421–4468.
- [2] C.T. Supuran, Carbonic anhydrases: novel therapeutic applications for inhibitors and activators, *Nat. Rev. Drug Discov.* 7 (2008) 168–181.
- [3] C. Lomelino, R. McKenna, Carbonic anhydrase inhibitors: a review on the progress of patent literature (2011–2016), *Expert Opin. Ther. Pat.* 26 (2016) 947–956.
- [4] C.T. Supuran, Advances in structure-based drug discovery of carbonic anhydrase inhibitors, *Expet Opin. Drug Discov.* 12 (2017) 61–88.
- [5] C.T. Supuran, G. De Simone, Carbonic Anhydrases as Biocatalysts: from Theory to Medical and Industrial Applications, Elsevier, 2015.
- [6] C.T. Supuran, How many carbonic anhydrase inhibition mechanisms exist? *J. Enzym. Inhib. Med. Chem.* 31 (2016) 345–360.
- [7] A. Waheed, W.S. Sly, Carbonic anhydrase XII functions in health and disease, *Gene* 623 (2017) 33–40.
- [8] C.T. Supuran, V. Alterio, A. Di Fiore, D.A. K. F. Carta, S.M. Monti, G. De Simone, Inhibition of carbonic anhydrase IX targets primary tumors, metastases, and cancer stem cells: three for the price of one, *Med. Res. Rev.* 38 (2018) 1799–1836. <https://doi.org/10.1002/med.21497>.
- [9] V. Alterio, D. Esposito, S.M. Monti, C.T. Supuran, G. De Simone, Crystal structure of the human carbonic anhydrase II adduct with 1-(4-sulfamoylphenylethyl)-2,4,6-triphenylpyridinium perchlorate, a membrane-impermeant, isoform selective inhibitor, *J. Enzym. Inhib. Med. Chem.* 33 (2018) 151–157.
- [10] S.M. Monti, C.T. Supuran, G. De Simone, Anticancer carbonic anhydrase inhibitors: a patent review (2008 - 2013), *Expert Opin. Ther. Pat.* 23 (2013) 737–749.
- [11] E. Bruno, M.R. Buemi, L. De Luca, S. Ferro, A.M. Monforte, C.T. Supuran, D. Vullo, G. De Sarro, E. Russo, R. Gitto, Vivo evaluation of selective carbonic anhydrase inhibitors as potential anticonvulsant agents, *ChemMedChem* 11 (2016) 1812–1818.
- [12] C.T. Supuran, Carbonic anhydrase inhibitors as emerging drugs for the treatment of obesity, *Expet Opin. Emerg. Drugs* 17 (2012) 11–15.
- [13] C.T. Supuran, A. Di Fiore, G. De Simone, Carbonic anhydrase inhibitors as emerging drugs for the treatment of obesity, *Expet Opin. Emerg. Drugs* 13 (2008) 383–392.
- [14] G. De Simone, A. Scozzafava, C.T. Supuran, Which carbonic anhydrases are targeted by the antiepileptic sulfonamides and sulfamates? *Chem. Biol. Drug Des.* 74 (2009) 317–321.
- [15] E. Ruusuvaari, K. Kaila, Carbonic anhydrases and brain pH in the control of neuronal excitability, *Subcell. Biochem.* 75 (2014) 271–290.
- [16] J.R. Casey, W.S. Sly, G.N. Shah, B.V. Alvarez, Bicarbonate homeostasis in excitable tissues: role of AE3 Cl⁻/HCO₃⁻ exchanger and carbonic anhydrase XIV interaction, *Am. J. Physiol. Cell Physiol.* 297 (2009) C1091–C1102.
- [17] M.R. Buemi, L. De Luca, S. Ferro, E. Bruno, M. Ceruso, C.T. Supuran, K. Pospíšilová, J. Brynda, P. Rezacová, R. Gitto, Carbonic anhydrase inhibitors: design, synthesis and structural characterization of new heteroaryl-N-carbonylbenzenesulfonamides targeting druggable human carbonic anhydrase isoforms, *Eur. J. Med. Chem.* 102 (2015) 223–232.
- [18] L. De Luca, F. Mancuso, S. Ferro, M.R. Buemi, A. Angeli, S. Del Prete, C. Capasso, C.T. Supuran, R. Gitto, Inhibitory effects and structural insights for a novel series of coumarin-based compounds that selectively target human CA IX and CA XII carbonic anhydrases, *Eur. J. Med. Chem.* 143 (2018) 276–282.
- [19] E. Bruno, M.R. Buemi, A. Di Fiore, L. De Luca, S. Ferro, A. Angeli, R. Cirilli, D. Sadutto, V. Alterio, S.M. Monti, C.T. Supuran, G. De Simone, R. Gitto, Probing molecular interactions between human carbonic anhydrases (hCAs) and a novel class of benzenesulfonamides, *J. Med. Chem.* 60 (2017) 4316–4326.
- [20] L. De Luca, S. Ferro, F.M. Damiano, C.T. Supuran, D. Vullo, A. Chimirri, R. Gitto, Structure-based screening for the discovery of new carbonic anhydrase VII inhibitors, *Eur. J. Med. Chem.* 71 (2014) 105–111.
- [21] R. Gitto, F.M. Damiano, P. Mader, L. De Luca, S. Ferro, C.T. Supuran, D. Vullo, J. Brynda, P. Rezacova, A. Chimirri, Synthesis, structure-activity relationship studies, and X-ray crystallographic analysis of arylsulfonamides as potent carbonic anhydrase inhibitors, *J. Med. Chem.* 55 (2012) 3891–3899.
- [22] R. Gitto, F.M. Damiano, L. De Luca, S. Ferro, D. Vullo, C.T. Supuran, A. Chimirri, Synthesis and biological profile of new 1,2,3,4-tetrahydroisoquinolines as selective carbonic anhydrase inhibitors, *Bioorg. Med. Chem.* 19 (2011) 7003–7007.
- [23] P. Mader, J. Brynda, R. Gitto, S. Agnello, P. Pächl, C.T. Supuran, A. Chimirri, P. Rezacova, Structural basis for the interaction between carbonic anhydrase and 1,2,3,4-tetrahydroisoquinolin-2-ylsulfonamides, *J. Med. Chem.* 54 (2011) 2522–2526.
- [24] R. Gitto, S. Agnello, S. Ferro, D. Vullo, C.T. Supuran, A. Chimirri, Identification of potent and selective human carbonic anhydrase VII (hCA VII) inhibitors, *ChemMedChem* 5 (2010) 823–826.
- [25] R. Gitto, S. Agnello, S. Ferro, L. De Luca, D. Vullo, J. Brynda, P. Mader,

- C.T. Supuran, A. Chimirri, Identification of 3,4-Dihydroisoquinoline-2(1H)-sulfonamides as potent carbonic anhydrase inhibitors: synthesis, biological evaluation, and enzyme–ligand X-ray studies, *J. Med. Chem.* 53 (2010) 2401–2408.
- [26] R. Gitto, S. Ferro, S. Agnello, L. De Luca, G. De Sarro, E. Russo, D. Vullo, C.T. Supuran, A. Chimirri, Synthesis and evaluation of pharmacological profile of 1-aryl-6,7-dimethoxy-3,4-dihydroisoquinoline-2(1H)-sulfonamides, *Bioorg. Med. Chem.* 17 (2009) 3659–3664.
- [27] R. Gitto, F.M. Damiano, L. De Luca, S. Ferro, D. Vullo, C.T. Supuran, A. Chimirri, Synthesis and biological profile of new 1,2,3,4-tetrahydroisoquinolines as selective carbonic anhydrase inhibitors, *Bioorg. Med. Chem.* 19 (2011) 7003–7007.
- [28] E. Russo, A. Constanti, G. Ferreri, R. Citraro, G. De Sarro, Nifedipine affects the anticonvulsant activity of topiramate in various animal models of epilepsy, *Neuropharmacology* 46 (2004) 865–878.
- [29] G. De Simone, V. Alterio, C.T. Supuran, Exploiting the hydrophobic and hydrophilic binding sites for designing carbonic anhydrase inhibitors, *Expert Opin. Drug Discov.* 8 (2013) 793–810.
- [30] A. Innocenti, D. Vullo, J. Pastorek, A. Scozzafava, S. Pastorekova, I. Nishimori, C.T. Supuran, Carbonic anhydrase inhibitors. Inhibition of transmembrane isozymes XII (cancer-associated) and XIV with anions, *Bioorg. Med. Chem. Lett* 17 (2007) 1532–1537.
- [31] I. Nishimori, D. Vullo, A. Innocenti, A. Scozzafava, A. Mastrolorenzo, C.T. Supuran, Carbonic anhydrase inhibitors: inhibition of the transmembrane isozyme XIV with sulfonamides, *Bioorg. Med. Chem. Lett* 15 (2005) 3828–3833.
- [32] I. Nishimori, D. Vullo, A. Innocenti, A. Scozzafava, A. Mastrolorenzo, C.T. Supuran, Carbonic anhydrase inhibitors. The mitochondrial isozyme VB as a new target for sulfonamide and sulfamate inhibitors, *J. Med. Chem.* 48 (2005) 7860–7866.
- [33] A. Di Fiore, E. Truppo, C.T. Supuran, V. Alterio, N. Dathan, F. Bootorabi, S. Parkkila, S.M. Monti, G. De Simone, Crystal structure of the C183S/C217S mutant of human CA VII in complex with acetazolamide, *Bioorg. Med. Chem. Lett* 20 (2010) 5023–5026.
- [34] M. Buonanno, A. Di Fiore, E. Langella, K. D'Ambrosio, C.T. Supuran, S.M. Monti, G. De Simone, The crystal structure of a hCA VII variant provides insights into the molecular determinants responsible for its catalytic behavior, *Int. J. Mol. Sci.* 19 (2018).
- [35] Z. Otwinowski, W. Minor, Processing of X-ray diffraction data collected in oscillation mode, *Methods Enzymol.* 276 (1997) 307–326.
- [36] A.E. Eriksson, T.A. Jones, A. Liljas, Refined structure of human carbonic anhydrase II at 2.0 Å resolution, *Proteins* 4 (1988) 274–282.
- [37] A.T. Brunger, P.D. Adams, G.M. Clore, W.L. DeLano, P. Gros, R.W. Grosse-Kunstleve, J.S. Jiang, J. Kuszewski, M. Nilges, N.S. Pannu, R.J. Read, L.M. Rice, T. Simonson, G.L. Warren, Crystallography & NMR system: a new software suite for macromolecular structure determination, *Acta Crystallogr. Sect. D Biol. Crystallogr.* 54 (1998) 905–921.
- [38] A.T. Brunger, Version 1.2 of the crystallography and NMR system, *Nat. Protoc.* 2 (2007) 2728–2733.
- [39] A. Di Fiore, A. Maresca, V. Alterio, C.T. Supuran, G. De Simone, Carbonic anhydrase inhibitors: X-ray crystallographic studies for the binding of N-substituted benzenesulfonamides to human isoform II, *Chem. Commun.* 47 (2011) 11636–11638.
- [40] A. Di Fiore, A. Maresca, C.T. Supuran, G. De Simone, Hydroxamate represents a versatile zinc binding group for the development of new carbonic anhydrase inhibitors, *Chem. Commun.* 48 (2012) 8838–8840.
- [41] A. Di Fiore, A. Vergara, M. Caterino, V. Alterio, S.M. Monti, J. Ombouma, P. Dumy, D. Vullo, C.T. Supuran, J.Y. Winum, G. De Simone, Hydroxylamine-O-sulfonamide is a versatile lead compound for the development of carbonic anhydrase inhibitors, *Chem. Commun.* 51 (2015) 11519–11522.
- [42] T.A. Jones, J.Y. Zou, S.W. Cowan, M. Kjeldgaard, Improved methods for building protein models in electron density maps and the location of errors in these models, *Acta Crystallogr. Section A, Found. Crystallogr.* 47 (Pt 2) (1991) 110–119.
- [43] A.W. Schuttelkopf, D.M. van Aalten, PRODRG: a tool for high-throughput crystallography of protein–ligand complexes, *Acta Crystallogr. Sect. D Biol. Crystallogr.* 60 (2004) 1355–1363.